Hindawi
Complexity
Volume 2023, Article ID 8880544, 13 pages
https://doi.org/10.1155/2023/8880544

Research Article

Modelization and Calibration of the Power-Law Distribution in Stock Market by Maximization of Varma Entropy

Chang Liu [1] **and Chuo Chang** [2]

[1]*School of Economics & Management, University of Science and Technology Beijing, Beijing 100083, China*
[2]*PBC School of Finance, Tsinghua University, Beijing 100083, China*

Correspondence should be addressed to Chang Liu; liuchang@ustb.edu.cn

Received 23 June 2023; Revised 13 September 2023; Accepted 20 September 2023; Published 30 September 2023

Academic Editor: Giacomo Fiumara

Proper description of the return distribution is crucial for investment practitioners. The underestimation of the tail risk may lead to severe consequences, even for assets with moderate fluctuations. However, many empirical studies found that the distribution tails of many financial assets drop off more slowly than the Gaussian distributions. Therefore, we intend to model and calibrate the heavy tails observed in financial fluctuations in this study. By maximizing the Varma entropy with value-at-risk and expected shortfall constraints, we obtain the probability distribution of stock return and observe that the tail of stock return distribution is a power law. Since the variance of the real stock portfolio may be a random variable, using the mean-VaR-ES constraints to maximize the Varma entropy effectively avoids the problem of assuming that the variance is a constant value under the traditional mean-variance constraint. Therefore, the deduced theoretical model would be more consistent with the real market. Using high-frequency data from China's stock markets, we calibrate our theoretical model and give the concrete form of probability density distribution $p(x)$ for different time intervals. The calibration results show that the tail of the stock return distribution is a power law with most of the power-law orders between −2 and −7. We prove the robustness of our results by calibrating the Varma entropy for S&P 500 of the USA stock market and different stock market indices in China's A-share market. Our research's findings not only offer a theoretical perspective for researchers but also give investing professionals a theoretical foundation on which to base their decisions.

1. Introduction

One of the most important conditions for every new financial investment is risk assessment. The underestimation of the tail risk may lead to severe consequences, even for assets with moderate fluctuations. Therefore, modeling the probability density distribution function accurately is crucial for financial investors.

The well-known Markowitz model assumes that the return on financial assets follows a Gaussian distribution. Nevertheless, it is observed that many stock indices do not follow the random walk [1] and the distribution tails of many financial assets drop off more slowly than the Gaussian distributions [2].

Various models have been proposed to improve the probability density distribution function of financial assets. Some scholars have proposed that empirical financial asset volatility should be a random quantity, not a constant one like in the Black–Scholes model [3]. For instance, ARCH models [4] use earlier time's real error term to describe the current error term's variance, and GARCH models [5] assume the variance of the error term to be an autoregressive moving average. These models are frequently used in the financial market to describe the time-varying and clustering volatility of financial assets.

Particularly, financial assets' power-law tails have been widely researched [6]. Mandelbrot [7] was the first to notice the power-law characteristics of financial asset price distributions. He modeled the logarithmic price increments with the Lévy flight, a stable distribution with a heavy-tailed distribution. A stable distribution is a sort of distribution that occurs when n independent and identically distributed

random variables are added together. Its characteristic is that its functional form remains unchanged for different values of n [8]. This process, according to Mandelbrot, might explain why the aggregated return distribution did not converge to the normal distribution predicted by the central limit theorem (CLT). Since then, a series of studies have been done analyzing theoretically or empirically the power-law tails of financial assets. Gopikrishnan et al. [9] used a sample of 40 million data in three major US stock markets to analyze the probability distribution of stock price changes. They discovered that the cumulative distribution had asymptotic power-law behavior with an exponent alpha of about 3, which is beyond the Lévy regime of $0 < \text{alpha} < 2$. The authors developed the so-called "inverse-cubic law" as a result of the stock markets' unexpected conduct. Plerou et al. [10] further studied the stock price fluctuations of individual companies for US stock markets systematically using stock price returns of time scales Δt from 5 minutes up to four years. Their observation showed that for time periods between 5 minutes and 16 days, a power-law decay may accurately depict the distribution's tails. The exponent of power law is between 2.5 and 4. Gopikrishnan et al. [11] conducted a parallel research using stock price indices. They observed that the distributions for the S&P 500 index for Δt shorter than 4 days exhibit a power-law asymptotic behavior, with the exponent around 3, well outside the stable Lévy regime $0 < \text{alpha} < 2$. NIKKEI index and Hang-Seng index also showed similar characteristics for time scales shorter than 4 days. Wątorek et al. [12] also identified the power-law behaviors of the tails using recent data on cryptocurrencies, exchange rates, and contracts for differences (CFDs). By contrasting their findings with those from past research, they concentrate on the fitted function parameters and how they evolve through time. Their findings showed that the so-called "inverse-cubic power law" was still a suitable global reference on time scales of up to a few minutes. In fact, comparable statistical traits were discovered by other researchers using information from different stock markets [13–19].

Therefore, for a stock market with a heavy tail in return distributions, it is necessary to use a new uncertainty measure that does not depend on a particular distribution. Entropy can be applied to measure uncertainty in probability theory. As a measure of diversity, the concept of entropy, especially the principles of maximum entropy, has been widely used in asset pricing and portfolio selection. The idea of entropy was initially used for portfolio selection by Philippatos and Wilson [20]. To optimize projected portfolio return and reduce portfolio entropy, they created the notions of individual entropy, joint entropy, and conditional entropy. The derived probability density distribution model matched the single-index and full covariance models. Since then, this field has achieved a lot of advancements. A mean-hybrid entropy model, for instance, was given by Xu et al. [21] to address the portfolio selection issue with asset risk resulting from both randomness and fuzziness. A mean-variance-skewness-entropy portfolio selection model (MVSEM) was created by Usta and Kantar [22] and outperformed conventional portfolio selection models in several out-of-sample experiments. To create a well-diversified asset portfolio, Jana et al. [23] incorporated an additional entropy objective function to the multiobjective portfolio-based model and the probabilistic mean value and variance of continuous distribution. A possibilistic mean-semivariance-entropy model including return, risk, transaction cost, and portfolio diversity level was developed by Zhang et al. [24] for multiperiod portfolio selection. Zhou et al. [25] introduced a portfolio selection model based on information entropy-incremental entropy-skewness (EESM), with information entropy measuring portfolio risk. They evaluated the performance of the EESM and found that the EESM performs well relative to traditional portfolio selection models. Huang [26] created two kinds of credibility-based fuzzy mean-entropy models: a straightforward approach for determining the average entropy front and a fuzzy average entropy model. By an information theoretical inference mechanism, Rödder et al. [27] established a novel theory for determining portfolio weights under maximum entropy and minimum relative entropy. Anton and Afloarei Nucu [28] investigated the credit default swap (CDS) and stock markets using the idea of entropy. Their empirical findings revealed a shift of risk entropy from the private to public sectors during the whole period and respectively. In summary, some studies used the entropy model to determine the portfolio weights, to identify the mean-entropic frontier, or to analyze portfolio selection with transaction costs. Some of them proposed different forms of entropy, such as the more generalized incremental entropy, hybrid entropy, or information entropy like the Renyi entropy [29, 30], please see [31] for a full review of the use of entropy in portfolio selection.

In this paper, we use Varma entropy constrained by value-at-risk and expected shortfall to build the probability density distribution of the financial assets return. We especially want to model and calibrate the heavy tails observed in the financial fluctuations. Since the tail region of stock price distribution follows the power law [32, 33], which is significantly different from the normal distribution, it does not make sense to discuss variance in these circumstances. In order to avoid the use of variance as a constraint when optimizing portfolio entropy, following [34, 35], we apply the value-at-risk and expected shortfall constraints instead of the variance constraint. In this way, the probability density distribution of return is more theoretically reasonable. It is found that the tail of stock return distribution is a power law by maximizing the Varma entropy with VaR and ES constraints. Then, we use high-frequency data of stock market indices from China to USA to calibrate the Varma entropy. With the real-world data, we find that the tail region of the stock market index return distribution is a power law with most of the power-law exponents between −2 and −7. With the increase of the time interval of return lag, the power-law exponents are mostly tending to decrease. This is consistent with the principle of maximum entropy as entropy tends to increase when the system approaches its equilibrium value. With the calculated value-at-risk and the expected shortfall values, we fix the four Lagrangian multipliers in the theoretically deduced probability density distribution and thus give the numerical form of our theoretical model for different stock market indices with different time intervals.

The rest of this paper is arranged as follows: In Section 2, using mean-VaR-ES constraints to maximize the Varma entropy, we deduce theoretically the probability density distribution of stock return. In Section 3, we use high-frequency data from China's stock market index to calibrate our theoretical model. In Section 4, we do the robustness tests using data from different stock markets. Finally, Section 5 draws conclusions.

2. Varma Entropy and the Power Law

In the real world, value-at-risk (VaR), developed by J.P. Morgan in the late 1980s [36], is a statistic in risk management that quantifies the risk of an asset portfolio into a numerical value. It describes the possible maximum loss over a certain period of time within a fixed confidence level. The value-at-risk (VaR) level K describes the greatest possible losses over a specific time frame with a $(1-\epsilon)$ level of confidence.

$$\mathbf{P}(\mathbf{x} \le \mathbf{K}) = \int_{-\infty}^{\mathbf{K}} \mathbf{p}(\mathbf{x})\mathbf{dx} = \boldsymbol{\epsilon}. \tag{1}$$

The concept of expected shortfall (ES) was first introduced by Rappoport and later developed by Artzner et al. [37, 38]. Expected shortfall is defined as the conditional expectation of loss when the loss exceeds the VaR threshold K, and it gauges how much one can lose on average in states beyond the selected level of VaR K. ES is derived by averaging all returns in the distribution that are less than the value-at-risk (VaR) level K during a certain time period with a $(1-\epsilon)$ degree of confidence:

$$\mathbf{ES} = \int_{-\infty}^{\mathbf{K}} \mathbf{x}\mathbf{p}(\mathbf{x})\mathbf{dx}, \tag{2}$$

where $p(x)$ represents the probability density distribution of the return and K represents the preselected VaR level.

The two-parameter Varma entropy [39] with continuous probability density distribution $p(x)$ is defined as follows:

$$\mathbf{H}_{\mathbf{ab}} = \frac{\mathbf{1}}{\mathbf{b}-\mathbf{a}} \mathbf{ln} \int_{-\infty}^{\infty} \mathbf{p}(\mathbf{x})^{\mathbf{a}+\mathbf{b}-\mathbf{1}} \mathbf{dx}, \tag{3}$$

with the normalization constraint:

$$\int_{-\infty}^{\infty} \mathbf{p}(\mathbf{x})\mathbf{dx} = \mathbf{1}. \tag{4}$$

Given the mean value of the portfolio μ, the global mean constraint takes the following form:

$$\mathbf{E}(\mathbf{x}) = \int_{-\infty}^{\infty} \mathbf{x}\mathbf{p}(\mathbf{x})\mathbf{dx} = \boldsymbol{\mu}. \tag{5}$$

We set K as the preselected VaR level and define the tail probability as

$$\mathbf{P}(\mathbf{x} \le \mathbf{K}) = \int_{-\infty}^{\mathbf{K}} \mathbf{p}(\mathbf{x})\mathbf{dx} = \boldsymbol{\epsilon}. \tag{6}$$

The expected shortfall may be stated as follows:

$$\mathbf{ES}(\mathbf{x} \le \mathbf{K}) = \int_{-\infty}^{\mathbf{K}} \mathbf{x}\mathbf{p}(\mathbf{x})\mathbf{dx} = \boldsymbol{\epsilon}\boldsymbol{\nu}. \tag{7}$$

The expected shortfall and tail probability may be formally rewritten as follows:

$$\mathbf{P}(\mathbf{x} \le \mathbf{K}) = \int_{-\infty}^{\mathbf{K}} \mathbf{g}^{\mathrm{Tail}}(\mathbf{x})\mathbf{p}(\mathbf{x})\mathbf{dx} = \boldsymbol{\epsilon}, \mathbf{g}^{\mathrm{Tail}}(\mathbf{x}) = \begin{cases} \mathbf{1}, \mathbf{x} \le \mathbf{K}, \\ \mathbf{0}, \mathbf{x} > \mathbf{K}, \end{cases} \tag{8}$$

$$\mathbf{ES}(\mathbf{x}\mathbf{I}_{\mathbf{x}\le\mathbf{K}}) = \int_{-\infty}^{\infty} \mathbf{g}^{\mathrm{ES}}(\mathbf{x})\mathbf{p}(\mathbf{x})\mathbf{dx} = \boldsymbol{\epsilon}\boldsymbol{\nu}, \mathbf{g}^{\mathrm{ES}}(\mathbf{x}) = \begin{cases} \mathbf{x}, \mathbf{x} \le \mathbf{K}, \\ \mathbf{0}, \mathbf{x} > \mathbf{K}. \end{cases} \tag{9}$$

In order to maximize the Varma entropy of equation (3), we construct the Lagrangian of the portfolio as follows:

$$\begin{aligned} \mathbf{L}^{\mathrm{Varma}} = \frac{\mathbf{1}}{\mathbf{b}-\mathbf{a}} \mathbf{ln} \int_{-\infty}^{\infty} \mathbf{p}(\mathbf{x})^{\mathbf{a}+\mathbf{b}-\mathbf{1}} \mathbf{dx} - \boldsymbol{\lambda}_{\mathbf{0}} \left(\int_{-\infty}^{\infty} \mathbf{p}(\mathbf{x})\mathbf{dx} - \mathbf{1} \right) - \boldsymbol{\lambda}_{\mathbf{1}} \left(\int_{-\infty}^{\infty} \mathbf{x}\mathbf{p}(\mathbf{x})\mathbf{dx} - \boldsymbol{\mu} \right) \\ - \boldsymbol{\gamma}^{\mathrm{Tail}} \left(\int_{-\infty}^{\infty} \mathbf{g}^{\mathrm{Tail}}(\mathbf{x})\mathbf{p}(\mathbf{x})\mathbf{dx} - \boldsymbol{\epsilon} \right) - \boldsymbol{\gamma}^{\mathrm{ES}} \left(\int_{-\infty}^{\infty} \mathbf{g}^{\mathrm{ES}}(\mathbf{x})\mathbf{p}(\mathbf{x})\mathbf{dx} - \boldsymbol{\epsilon}\boldsymbol{\nu} \right). \end{aligned} \tag{10}$$

The Lagrangian will be maximized when its functional variation with regard to the unidentified probability density distribution $p(x)$ is zero:

$$\delta \mathbf{L} = \int_{-\infty}^{\infty} \left[\frac{\mathbf{a}+\mathbf{b}-\mathbf{1}}{\mathbf{b}-\mathbf{a}} \frac{\mathbf{p}(\mathbf{x})^{\mathbf{a}+\mathbf{b}-\mathbf{2}}}{\int_{-\infty}^{\infty} \mathbf{p}(\mathbf{x})^{\mathbf{a}+\mathbf{b}-\mathbf{1}} \mathbf{dx}} - \boldsymbol{\lambda}_{\mathbf{0}} - \boldsymbol{\lambda}_{\mathbf{1}}\mathbf{x} - \boldsymbol{\gamma}^{\mathrm{Tail}}\mathbf{g}^{\mathrm{Tail}} - \boldsymbol{\gamma}^{\mathrm{ES}}\mathbf{g}^{\mathrm{ES}}(\mathbf{x}) \right] \boldsymbol{\delta}\mathbf{p}(\mathbf{x}) = \mathbf{0}. \tag{11}$$

Solving the above formula and using the mean-VaR-ES constraints, we may derive the probability density distribution as follows:

$$\mathbf{p}(\mathbf{x}) = \left[\frac{\mathbf{b}-\mathbf{a}}{\mathbf{a}+\mathbf{b}-\mathbf{1}} \int_{-\infty}^{\infty} \mathbf{p}(\mathbf{x})^{\mathbf{a}+\mathbf{b}-\mathbf{1}} \mathbf{dx} \left(\boldsymbol{\lambda}_{\mathbf{0}} + \boldsymbol{\lambda}_{\mathbf{1}}\mathbf{x} + \boldsymbol{\gamma}^{\mathrm{Tail}}\mathbf{g}^{\mathrm{Tail}} + \boldsymbol{\gamma}^{\mathrm{ES}}\mathbf{g}^{\mathrm{ES}}(\mathbf{x}) \right) \right]^{(\mathbf{1}/\mathbf{a}+\mathbf{b}-\mathbf{2})}. \tag{12}$$

In accordance with the mean-VaR-ES requirements, we may rewrite the probability density distribution as follows:

$$\mathbf{p}(\mathbf{x}) = \left(\overline{\boldsymbol{\lambda}_{\mathbf{0}}} + \overline{\boldsymbol{\lambda}_{\mathbf{1}}}\mathbf{x} + \overline{\boldsymbol{\gamma}}^{\mathrm{Tail}}\mathbf{g}^{\mathrm{Tail}} + \overline{\boldsymbol{\gamma}}^{\mathrm{ES}}\mathbf{g}^{\mathrm{ES}}(\mathbf{x}) \right)^{(\mathbf{1}/\mathbf{a}+\mathbf{b}-\mathbf{2})}, \tag{13}$$

where $\overline{\lambda_0} = N\lambda_0$, $\overline{\lambda_1} = N\lambda_1$, $\overline{\gamma}^{\mathrm{Tail}} = N\gamma^{\mathrm{Tail}}$, and $\overline{\gamma}^{\mathrm{ES}} = N\gamma^{\mathrm{ES}}$, and $N = [(b-a)/(a+b-1)\int_{-\infty}^{\infty} p(x)^{a+b-1}\mathrm{d}x]$.

The unity requirement (4) of the probability density function may be expressed as follows using the probability density distribution under the above mean-VaR-ES constraints:

$$\begin{aligned} &\int_{-\infty}^{\mathbf{K}} \left(\overline{\boldsymbol{\lambda}_{\mathbf{0}}} + \overline{\boldsymbol{\lambda}_{\mathbf{1}}}\mathbf{x} + \overline{\boldsymbol{\gamma}}^{\mathrm{Tail}} + \mathbf{x}\overline{\boldsymbol{\gamma}}^{\mathrm{ES}} \right)^{(\mathbf{1}/\mathbf{a}+\mathbf{b}-\mathbf{2})} \mathbf{dx} \\ &+ \int_{\mathbf{K}}^{\infty} \left(\overline{\boldsymbol{\lambda}_{\mathbf{0}}} + \overline{\boldsymbol{\lambda}_{\mathbf{1}}}\mathbf{x} \right)^{(\mathbf{1}/\mathbf{a}+\mathbf{b}-\mathbf{2})} \mathbf{dx} = \mathbf{1}. \end{aligned} \tag{14}$$

If Varma entropy's two parameters satisfy $1 < a + b < 2$, we can integrate out equation (14) as follows:

$$\frac{\mathbf{a}+\mathbf{b}-\mathbf{2}}{\mathbf{a}+\mathbf{b}-\mathbf{1}} \left[\frac{\mathbf{1}}{\overline{\boldsymbol{\lambda}_{\mathbf{1}}} + \overline{\boldsymbol{\gamma}}^{\mathrm{ES}}} \left[\overline{\boldsymbol{\lambda}_{\mathbf{0}}} + \overline{\boldsymbol{\gamma}}^{\mathrm{Tail}} + \mathbf{K}\left(\overline{\boldsymbol{\lambda}_{\mathbf{1}}} + \overline{\boldsymbol{\gamma}}^{\mathrm{ES}} \right) \right]^{(\mathbf{a}+\mathbf{b}-\mathbf{1}/\mathbf{a}+\mathbf{b}-\mathbf{2})} - \frac{\mathbf{1}}{\overline{\boldsymbol{\lambda}_{\mathbf{1}}}} \left[\overline{\boldsymbol{\lambda}_{\mathbf{0}}} + \overline{\boldsymbol{\lambda}_{\mathbf{1}}}\mathbf{K} \right]^{(\mathbf{a}+\mathbf{b}-\mathbf{1}/\mathbf{a}+\mathbf{b}-\mathbf{2})} \right] = \mathbf{1}. \tag{15}$$

Using the probability density distribution with the mean-VaR-ES restrictions (13), we can rewrite the mean constraint (5) as follows:

$$\mathbf{E}(\mathbf{x}) = \int_{-\infty}^{\infty} \mathbf{x} \left(\overline{\boldsymbol{\lambda}_{\mathbf{0}}} + \overline{\boldsymbol{\lambda}_{\mathbf{1}}}\mathbf{x} + \overline{\boldsymbol{\gamma}}^{\mathrm{Tail}}\mathbf{g}^{\mathrm{Tail}} + \overline{\boldsymbol{\gamma}}^{\mathrm{ES}}\mathbf{g}^{\mathrm{ES}}(\mathbf{x}) \right)^{(\mathbf{1}/\mathbf{a}+\mathbf{b}-\mathbf{2})} \mathbf{dx} = \boldsymbol{\mu}. \tag{16}$$

If Varma entropy's two parameters satisfy $3/2 < a + b < 2$, we can have

$$\begin{aligned} &\frac{\mathbf{a}+\mathbf{b}-\mathbf{2}}{\mathbf{a}+\mathbf{b}-\mathbf{1}} \left\{ \mathbf{K} \left[\frac{\mathbf{1}}{\overline{\boldsymbol{\lambda}_{\mathbf{1}}} + \overline{\boldsymbol{\gamma}}^{\mathrm{ES}}} \left[\overline{\boldsymbol{\lambda}_{\mathbf{0}}} + \overline{\boldsymbol{\gamma}}^{\mathrm{Tail}} + \mathbf{K}\left(\overline{\boldsymbol{\lambda}_{\mathbf{1}}} + \overline{\boldsymbol{\gamma}}^{\mathrm{ES}} \right) \right]^{(\mathbf{a}+\mathbf{b}-\mathbf{1}/\mathbf{a}+\mathbf{b}-\mathbf{2})} - \frac{\mathbf{1}}{\overline{\boldsymbol{\lambda}_{\mathbf{1}}}} \left[\overline{\boldsymbol{\lambda}_{\mathbf{0}}} + \overline{\boldsymbol{\lambda}_{\mathbf{1}}}\mathbf{K} \right]^{(\mathbf{a}+\mathbf{b}-\mathbf{1}/\mathbf{a}+\mathbf{b}-\mathbf{2})} \right] \right. \\ &\left. - \frac{\mathbf{a}+\mathbf{b}-\mathbf{2}}{\mathbf{2a}+\mathbf{2b}-\mathbf{3}} \left[\frac{\mathbf{1}}{\left(\overline{\boldsymbol{\lambda}_{\mathbf{1}}} + \overline{\boldsymbol{\gamma}}^{\mathrm{ES}} \right)^{\mathbf{2}}} \left[\overline{\boldsymbol{\lambda}_{\mathbf{0}}} + \overline{\boldsymbol{\gamma}}^{\mathrm{Tail}} + \mathbf{K}\left(\overline{\boldsymbol{\lambda}_{\mathbf{1}}} + \overline{\boldsymbol{\gamma}}^{\mathrm{ES}} \right) \right]^{(\mathbf{2a}+\mathbf{2b}-\mathbf{3}/\mathbf{a}+\mathbf{b}-\mathbf{2})} - \frac{\mathbf{1}}{\overline{\boldsymbol{\lambda}_{\mathbf{1}}^{\mathbf{2}}}} \left[\overline{\boldsymbol{\lambda}_{\mathbf{0}}} + \overline{\boldsymbol{\lambda}_{\mathbf{1}}}\mathbf{K} \right]^{(\mathbf{2a}+\mathbf{2b}-\mathbf{3}/\mathbf{a}+\mathbf{b}-\mathbf{2})} \right] \right\}. \end{aligned} \tag{17}$$

We may write the tail probability constraint (8) by using the probability density distribution under the mean-VaR-ES requirements (13) as follows:

$$\mathbf{P}(\mathbf{x} \le \mathbf{K}) = \int_{-\infty}^{\mathbf{K}} \left(\overline{\boldsymbol{\lambda}_0} + \overline{\boldsymbol{\lambda}_1}\mathbf{x} + \overline{\boldsymbol{\gamma}}^{\mathrm{Tail}}\mathbf{g}^{\mathrm{Tail}} + \overline{\boldsymbol{\gamma}}^{\mathrm{ES}}\mathbf{g}^{\mathrm{ES}}(\mathbf{x})\right)^{(\mathbf{1/a+b-2})} \mathbf{dx} = \boldsymbol{\epsilon}. \tag{18}$$

If Varma entropy's two parameters satisfy $1 < a + b < 2$, we have

$$\frac{\mathbf{a+b-2}}{\mathbf{a+b-1}} \frac{\mathbf{1}}{\overline{\boldsymbol{\lambda}_1} + \overline{\boldsymbol{\gamma}}^{\mathrm{ES}}} \left[\overline{\boldsymbol{\lambda}_0} + \overline{\boldsymbol{\gamma}}^{\mathrm{Tail}} + \mathbf{K}\left(\overline{\boldsymbol{\lambda}_1} + \overline{\boldsymbol{\gamma}}^{\mathrm{ES}}\right)\right]^{(\mathbf{a+b-1/a+b-2})} = \boldsymbol{\epsilon}. \tag{19}$$

By making use of equation (13), the expected shortfall constraint (9) can be expressed as follows:

$$\mathbf{ES}(\mathbf{x} \le \mathbf{K}) = \int_{-\infty}^{\mathbf{K}} \mathbf{x}\left(\overline{\boldsymbol{\lambda}_0} + \overline{\boldsymbol{\lambda}_1}\mathbf{x} + \overline{\boldsymbol{\gamma}}^{\mathrm{Tail}}\mathbf{g}^{\mathrm{Tail}} + \overline{\boldsymbol{\gamma}}^{\mathrm{ES}}\mathbf{g}^{\mathrm{ES}}(\mathbf{x})\right)^{(\mathbf{1/a+b-2})} \mathbf{dx} = \boldsymbol{\epsilon}\mathbf{v}. \tag{20}$$

If Varma entropy's two parameters satisfy $3/2 < a + b < 2$, we have

$$\begin{aligned} &\frac{\mathbf{a+b-2}}{\mathbf{a+b-1}} \left\{ \frac{\mathbf{1}}{\overline{\boldsymbol{\lambda}_1} + \overline{\boldsymbol{\gamma}}^{\mathrm{ES}}} \left[\overline{\boldsymbol{\lambda}_0} + \overline{\boldsymbol{\gamma}}^{\mathrm{Tail}} + \mathbf{K}\left(\overline{\boldsymbol{\lambda}_1} + \overline{\boldsymbol{\gamma}}^{\mathrm{ES}}\right)\right]^{(\mathbf{a+b-1/a+b-2})} \right. \\ &\left. - \frac{\mathbf{a+b-2}}{\mathbf{2a+2b-3}} \frac{\mathbf{1}}{\left(\overline{\boldsymbol{\lambda}_1} + \overline{\gamma}^{\mathrm{ES}}\right)^{\mathbf{2}}} \left[\overline{\boldsymbol{\lambda}_0} + \overline{\gamma}^{\mathrm{Tail}} + \mathbf{K}\left(\overline{\boldsymbol{\lambda}_1} + \overline{\boldsymbol{\gamma}}^{\mathrm{ES}}\right)\right]^{(\mathbf{2a+2b-3/a+b-2})} \right\} = \boldsymbol{\epsilon}\mathbf{v}. \end{aligned} \tag{21}$$

In order to build up all of the algebraic equations (15), (17), (19), and (21) simultaneously, we restricted the specified parameters of the Varma entropy as follows:

$$\frac{\mathbf{3}}{\mathbf{2}} < \mathbf{a} + \mathbf{b} < \mathbf{2}. \tag{22}$$

Setting:

$$\mathbf{a} + \mathbf{b} = \frac{\mathbf{2q-1}}{\mathbf{q}}. \tag{23}$$

The limiting condition (22) gives

$$\mathbf{q} \ge \mathbf{2}. \tag{24}$$

Therefore, $p(x)$ with mean-VaR-ES constraints may be altered to read as follows:

$$\mathbf{p}(\mathbf{x}) = \frac{\mathbf{1}}{\left(\overline{\boldsymbol{\lambda}_0} + \overline{\boldsymbol{\lambda}_1}\mathbf{x} + \overline{\gamma}^{\mathrm{Tail}}\mathbf{g}^{\mathrm{Tail}} + \overline{\boldsymbol{\gamma}}^{\mathrm{ES}}\mathbf{g}^{\mathrm{ES}}(\mathbf{x})\right)^{\mathbf{q}}}, \tag{25}$$

which shows that the probability density distribution with mean-VaR-ES constraints is a power law.

Utilizing the above equation (25), the distribution parameters' constraint (15) becomes

$$\frac{\mathbf{1}}{\mathbf{1-q}} \left[\frac{\mathbf{1}}{\overline{\boldsymbol{\lambda}_1} + \overline{\boldsymbol{\gamma}}^{\mathrm{ES}}} \left[\overline{\boldsymbol{\lambda}_0} + \overline{\boldsymbol{\gamma}}^{\mathrm{Tail}} + \mathbf{K}\left(\overline{\boldsymbol{\lambda}_1} + \overline{\boldsymbol{\gamma}}^{\mathrm{ES}}\right)\right]^{(\mathbf{1-q})} - \frac{\mathbf{1}}{\overline{\boldsymbol{\lambda}_1}} \left[\overline{\boldsymbol{\lambda}_0} + \overline{\boldsymbol{\lambda}_1}\mathbf{K}\right]^{(\mathbf{1-q})} \right] = \mathbf{1}. \tag{26}$$

Utilizing the equation (25), the distribution parameters' constraint (17) becomes

$$\frac{1}{1-q}\left\{K\left[\frac{1}{\overline{\lambda_1}+\overline{\gamma}^{ES}}\left[\overline{\lambda_0}+\overline{\gamma}^{Tail}+K\left(\overline{\lambda_1}+\overline{\gamma}^{ES}\right)\right]^{(1-q)}-\frac{1}{\overline{\lambda_1}}\left[\overline{\lambda_0}+\overline{\lambda_1}K\right]^{(1-q)}\right]\right.$$
$$\left.-\frac{1}{2-q}\left[\frac{1}{\left(\overline{\lambda_1}+\overline{\gamma}^{ES}\right)^2}\left[\overline{\lambda_0}+\overline{\gamma}^{Tail}+K\left(\overline{\lambda_1}+\overline{\gamma}^{ES}\right)\right]^{(2-q)}-\frac{1}{\overline{\lambda_1}^2}\left[\overline{\lambda_0}+\overline{\lambda_1}K\right]^{(2-q)}\right]\right\}=\mu. \tag{27}$$

Utilizing the equation (25), the distribution parameters' constraint (19) can be written as follows:

$$\frac{1}{1-q}\frac{1}{\overline{\lambda_1}+\overline{\gamma}^{ES}}\left[\overline{\lambda_0}+\overline{\gamma}^{Tail}+K\left(\overline{\lambda_1}+\overline{\gamma}^{ES}\right)\right]^{(1-q)}=\epsilon. \tag{28}$$

Utilizing the equation (25), the distribution parameters' constraint (21) can be written as follows:

$$\frac{1}{1-q}\left\{\frac{1}{\overline{\lambda_1}+\overline{\gamma}^{ES}}\left[\overline{\lambda_0}+\overline{\gamma}^{Tail}+K\left(\overline{\lambda_1}+\overline{\gamma}^{ES}\right)\right]^{(1-q)}-\frac{1}{2-q}\frac{1}{\left(\overline{\lambda_1}+\overline{\gamma}^{ES}\right)^2}\left[\overline{\lambda_0}+\overline{\gamma}^{Tail}+K\left(\overline{\lambda_1}+\overline{\gamma}^{ES}\right)\right]^{(2-q)}\right\}=\epsilon\nu. \tag{29}$$

It can be seen that if the Varma entropy's parameters and mean-VaR-ES constraints are given, then we can use the equations (26)–(29) to jointly determine $\overline{\lambda_0}$, $\overline{\lambda_1}$, $\overline{\gamma}^{Tail}$, and $\overline{\gamma}^{ES}$ in the probability density distribution $p(x)$ in equation (25).

3. Calibrating Varma Entropy

In the theoretical part, we have theoretically deduced that the tail region of the return distribution is a power-law distribution by maximizing Varma information entropy with mean-VaR-ES constraints. In this section, we will use real-world data to calibrate our theoretical model.

3.1. Data. For the purpose of risk management, studying the stock market index has a higher significance than studying individual stocks. The unsystematic risk of individual stocks can be hedged away by appropriate diversified investment. However, the systemic risk caused by the fluctuation of the stock market index cannot be reduced or eliminated through decentralized investment, since the systematic risk has an overall impact on the whole market. Therefore, in this paper, we choose the stock market index to study the characteristics of the return distribution of the stock market.

Given that China has become the second largest economy in the world and is the largest emerging economy [40], we use the stock market index from China to calibrate the model. In order to reflect the overall situation of China's stock market and in line with previous research, the Shanghai and Shenzhen 300 index (CSI 300 index) is utilized. The CSI 300 index is a capitalization-weighted stock market index reflecting the stock markets of Shanghai and Shenzhen, which was jointly released by China Securities Index Co., Ltd. and Shanghai and Shenzhen stock exchanges in April 2005. The stock scope of the CSI 300 index is comprehensively determined according to the market value and tradable market value of the stock, which has nothing to do with the industry of the company. The CSI 300 index covers most of the circulating stocks of Shanghai and Shenzhen stock markets and comprehensively covers large blue chip companies and small- and medium-sized companies. It is the stock market index used by most scholars to study China's stock market.

3.2. Market Return. The data we use are intraday high-frequency data. We have downloaded the high-frequency stock index with a data frequency of 1 minute using the Wind database and calculated the logarithmic rate of return for the stock market index $Z_{\Delta t}$ using the following equation:

$$Z_{\Delta t}(t) \equiv \ln S(t+\Delta t) - \ln S(t), \tag{30}$$

where $S(t)$ represents the stock market index at time t and $S(t+\Delta t)$ represents the stock market index at time $t+\Delta t$. In this paper, we study the stock return of short-time interval. We choose the time interval $\Delta t = 10$, 20, 30, 40, 50, 60, 70, and 80 minutes, respectively, to calculate the stock price return of the corresponding time interval. 10 minutes are close to the minimum time interval for completing a transaction. Our research is mainly based on risk management rather than high-frequency trading, so it is of little significance to study smaller time intervals.

In Table 1, we list the descriptive statistics of our sample, including the sample size, the mean value, the standard deviation, and the minimum and maximum of the data. The sample period starts from January 2018 to the end of 2018. It can be seen that the stock market may indeed fluctuate

Table 1: Descriptive statistics.

Variable	Sample	Mean	Standard deviation	Minimum (%)	Maximum (%)
$\Delta t = 10$ min	53460	-1.85×10^{-5}	2.05×10^{-3}	−1.56	1.26
$\Delta t = 20$ min	48600	-7.88×10^{-5}	2.89×10^{-3}	−2.51	1.67
$\Delta t = 30$ min	43740	-1.26×10^{-4}	3.57×10^{-3}	−2.64	1.83
$\Delta t = 40$ min	38880	-1.75×10^{-4}	4.13×10^{-3}	−3.02	2.43
$\Delta t = 50$ min	34020	-2.57×10^{-4}	4.65×10^{-3}	−3.31	2.39
$\Delta t = 60$ min	29160	-3.34×10^{-4}	5.15×10^{-3}	−3.41	2.43
$\Delta t = 70$ min	24300	-3.60×10^{-4}	5.58×10^{-3}	−3.45	2.71
$\Delta t = 80$ min	19440	-3.50×10^{-4}	6.00×10^{-3}	−3.61	2.88

[1]The data used are CSI 300 index of 2018 obtained from Wind.

greatly within a short period of time. For $\Delta t = 10$ minutes, the largest decline of the CSI 300 index reached 1.56%. In 80 minutes, the largest decline of the CSI 300 index reached 3.61%. It can be seen that the research on the stock return of short-time interval and the effective management of the risk of intraday fluctuation in the stock market are of great significance in the field of risk management.

In Table 2, we use skewness, kurtosis, Jarque–Bera test, Kolmogorov–Smirnov test, and Anderson–Darling test, respectively, to test whether the return distribution obeys the normal distribution. It can be seen from Table 2 that the skewness of the sample data is above 0, and there is positive bias; the sample data have leptokurtosis; Jarque–Bera test, Kolmogorov–Smirnov test, and Anderson–Darling test all significantly reject the original assumption that the sample data obey the normal distribution. That is, the return distribution of short-time interval does not obey the normal distribution.

3.3. Power Law and Calibrating Varma Entropy. Now, we analyze the tail region of the return distribution using data from the CSI 300 index. We first use the log-log diagram to exhibit the power-law relationship between the rate of return Z and the probability distribution $P(Z)$. When there is a power-law relationship between the rate of return Z and the probability distribution $P(Z)$, $\log Z$ and $\log P(Z)$ should have a linear relationship. As shown in Figure 1, the log-log plot of the CSI 300 index directly reflects the linear relationship between $\log Z$ and $\log P(Z)$. That is, the tail region of the short-time interval return distribution obeys the power-law distribution.

Following [12], we also transformed the return $Z_{\Delta t}(t)$ into the normalized form $\overline{Z_{\Delta t}(t)}$ according to

$$\overline{\mathbf{Z}_{\Delta \mathbf{t}}(\mathbf{t})} = \frac{\mathbf{Z}_{\Delta \mathbf{t}}(\mathbf{t}) - \boldsymbol{\mu}_{\mathbf{Z}_{\Delta \mathbf{t}}}}{\boldsymbol{\sigma}_{\mathbf{Z}_{\Delta \mathbf{t}}}}, \tag{31}$$

where Δt is the time interval, $\mu_{Z_{\Delta t}}$ is the mean of $Z_{\Delta t}(t)$, and $\sigma_{Z_{\Delta t}}$ is the standard deviation of $Z_{\Delta t}(t)$. The log-log plot of the probability distribution of normalized return $\overline{Z_{\Delta t}(t)}$ with different time intervals for CSI300 is shown in Figure 2.

We fit the tail region of the return distribution of CSI 300 index data using MATLAB. The power-law exponent and the R^2 are exhibited in Table 3. As can be seen in Table 3, the power-law exponents are between −7 and −2 with very high R^2. This indicates that the power-law distribution can describe the tail region of the short-time interval return distribution well, which is consistent with the conclusion drawn from the log-log graph. With increasing the return lags (from 10 to 80 min), the distribution tail power-law exponents are mostly expected to decrease.

We calculate the value-at-risk and the expected shortfall of CSI300 within 5% confidence level. Solving equations (26)–(29) jointly, we fix the four Lagrangian multipliers $\overline{\lambda_0}$, $\overline{\lambda_1}$, $\overline{\gamma}^{\text{Tail}}$, and $\overline{\gamma}^{\text{ES}}$ in the probability density distribution under the mean-VaR-ES constraints (25). The numerical results of the four Lagrangian multipliers are shown in Table 3.

Having obtained the Lagrangian multipliers, we can write the numerical form of probability density distribution for different stock market indexes with different time intervals.

For $\Delta t = 10$ min, the probability density distribution $p(Z)$ of CSI300 is

$$\mathbf{p}(\mathbf{Z}) = \left[\mathbf{0.36} + \mathbf{32.34Z} - \mathbf{0.37g}^{\text{Tail}}(\mathbf{Z}) - \mathbf{169.21g}^{\text{ES}}(\mathbf{Z})\right]^{-\mathbf{4.55}}. \tag{32}$$

For $\Delta t = 20$ min, the probability density distribution $p(Z)$ of CSI300 is

$$\mathbf{p}(\mathbf{Z}) = \left[\mathbf{0.51} + \mathbf{20.70Z} - \mathbf{0.29g}^{\text{Tail}}(\mathbf{Z}) - \mathbf{99.28g}^{\text{ES}}(\mathbf{Z})\right]^{-\mathbf{6.45}}. \tag{33}$$

For $\Delta t = 30$ min, the probability density distribution $p(Z)$ of CSI300 is

$$\mathbf{p}(\mathbf{Z}) = \left[\mathbf{0.41} + \mathbf{20.91Z} - \mathbf{0.41g}^{\text{Tail}}(\mathbf{Z}) - \mathbf{106.09g}^{\text{ES}}(\mathbf{Z})\right]^{-\mathbf{4.66}}. \tag{34}$$

For $\Delta t = 40$ min, the probability density distribution $p(Z)$ of CSI300 is

$$\mathbf{p}(\mathbf{Z}) = \left[\mathbf{0.33} + \mathbf{21.61Z} - \mathbf{0.24g}^{\text{Tail}}(\mathbf{Z}) + \mathbf{9.08g}^{\text{ES}}(\mathbf{Z})\right]^{-\mathbf{3.35}}. \tag{35}$$

For $\Delta t = 50$ min, the probability density distribution $p(Z)$ of CSI300 is

$$\mathbf{p}(\mathbf{Z}) = \left[\mathbf{0.39} + \mathbf{18.42Z} - \mathbf{0.59g}^{\text{Tail}}(\mathbf{Z}) - \mathbf{104.64g}^{\text{ES}}(\mathbf{Z})\right]^{-\mathbf{3.85}}. \tag{36}$$

For $\Delta t = 60$ min, the probability density distribution $p(Z)$ of CSI300 is

Table 2: Normality tests.

Variable	Skewness	Kurtosis	P value		
			Jarque–Bera test	Kolmogorov–Smirnov test	Anderson–Darling test
$\Delta t = 10$ min	0.30	5.44	$P < 0.001$	$P < 0.001$	$P < 0.001$
$\Delta t = 20$ min	0.19	5.44	$P < 0.001$	$P < 0.001$	$P < 0.001$
$\Delta t = 30$ min	0.24	5.29	$P < 0.001$	$P < 0.001$	$P < 0.001$
$\Delta t = 40$ min	0.25	5.14	$P < 0.001$	$P < 0.001$	$P < 0.001$
$\Delta t = 50$ min	0.20	5.13	$P < 0.001$	$P < 0.001$	$P < 0.001$
$\Delta t = 60$ min	0.19	5.13	$P < 0.001$	$P < 0.001$	$P < 0.001$
$\Delta t = 70$ min	0.19	4.87	$P < 0.001$	$P < 0.001$	$P < 0.001$
$\Delta t = 80$ min	0.19	4.46	$P < 0.001$	$P < 0.001$	$P < 0.001$

[1]The data used are CSI 300 index of 2018 obtained from Wind.

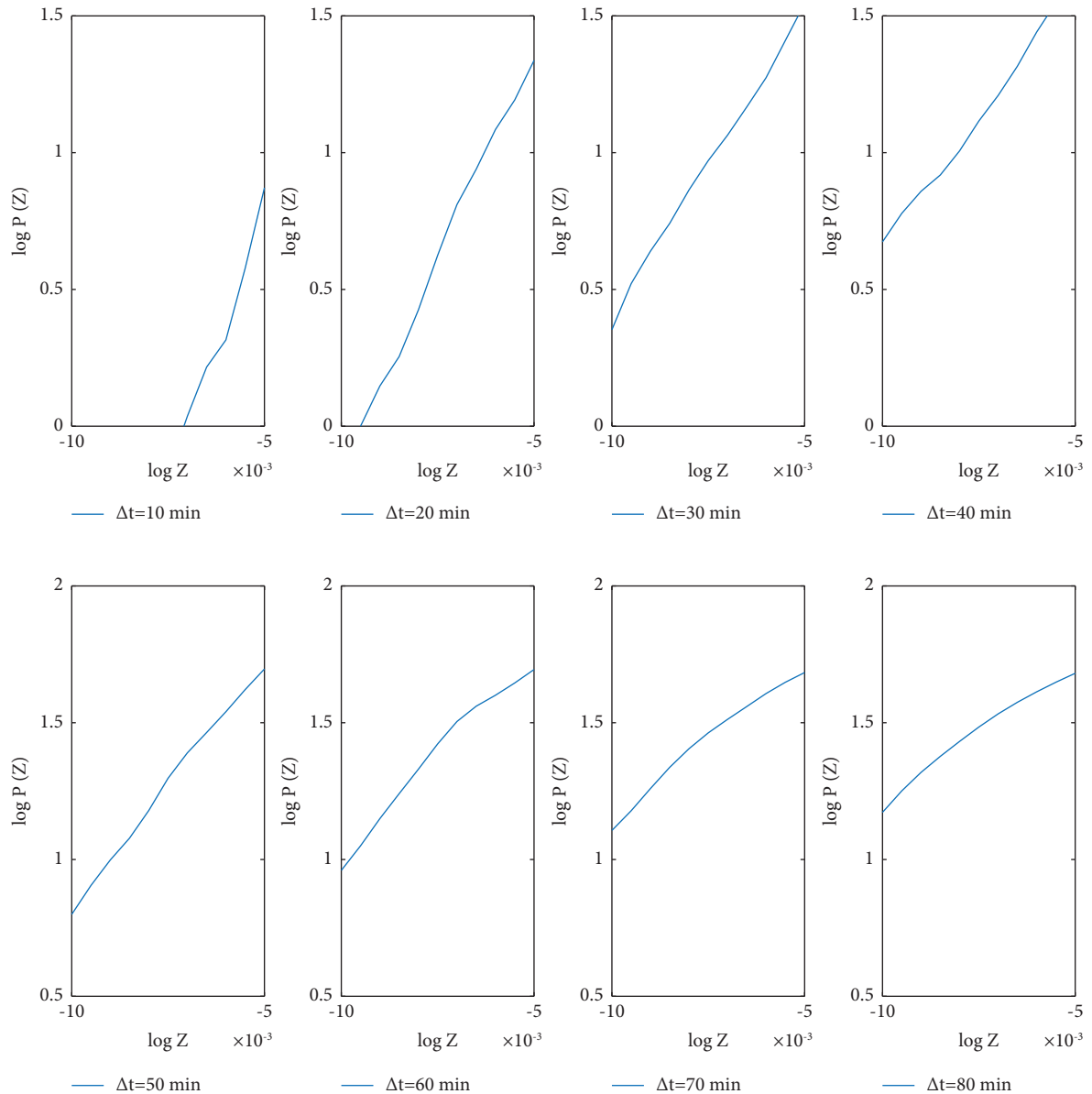

Figure 1: Log-log diagram of the probability distribution of return Z with different time intervals for CSI300.

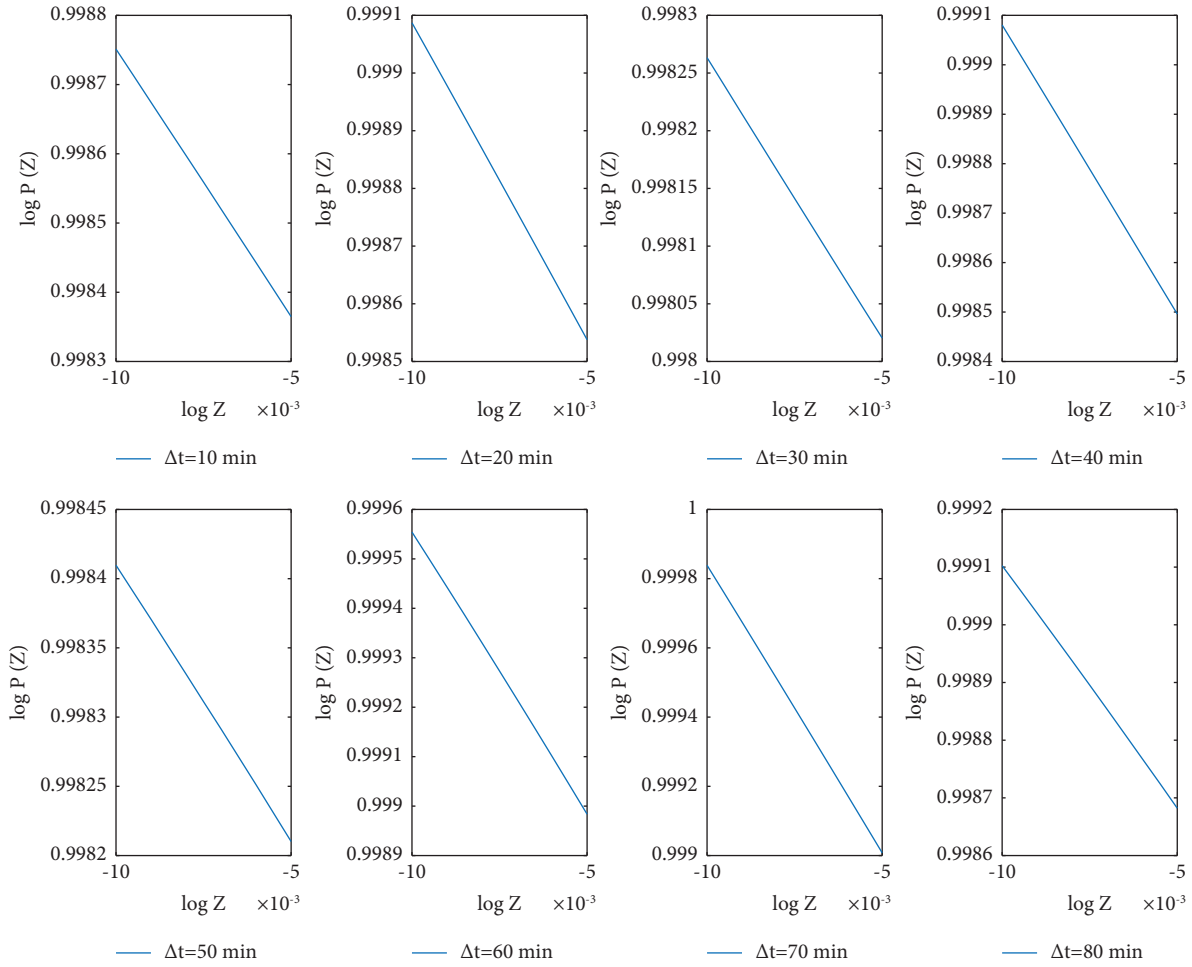

Figure 2: Log-log diagram of the probability distribution of normalized return $\overline{Z_{\Delta t}(t)}$ with different time intervals for CSI300.

Table 3: Power-law distribution test in the tail region of return distribution of CSI 300 index.

Variable	R^2	q	$\overline{\lambda_0}$	$\overline{\lambda_1}$	$\overline{\gamma}^{\text{Tail}}$	$\overline{\gamma}^{\text{ES}}$
$\Delta t = 10$ min	0.9106	4.55	0.36	32.34	−0.37	−169.21
$\Delta t = 20$ min	0.9881	6.45	0.51	20.70	−0.29	−99.28
$\Delta t = 30$ min	0.9880	4.66	0.41	20.91	−0.41	−106.09
$\Delta t = 40$ min	0.9943	3.35	0.33	21.61	−0.24	9.08
$\Delta t = 50$ min	0.9981	3.85	0.39	18.42	−0.59	−104.64
$\Delta t = 60$ min	0.9970	3.67	0.38	17.49	−0.64	−99.89
$\Delta t = 70$ min	0.9895	2.83	0.32	19.32	0.13	50.15
$\Delta t = 80$ min	0.9866	2.38	0.30	22.66	−1.59	−174.47

[1]The data used are CSI 300 index of 2018 obtained from Wind.

$$\mathbf{p}(\mathbf{Z}) = \left[\mathbf{0.38} + \mathbf{17.49Z} - \mathbf{0.64g}^{\text{Tail}}(\mathbf{Z}) - \mathbf{99.89g}^{\text{ES}}(\mathbf{Z})\right]^{-\mathbf{3.67}}. \tag{37}$$

For $\Delta t = 70$ min, the probability density distribution $p(Z)$ of CSI300 is

$$\mathbf{p}(\mathbf{Z}) = \left[\mathbf{0.32} + \mathbf{19.32Z} + \mathbf{0.13g}^{\text{Tail}}(\mathbf{Z}) + \mathbf{50.15g}^{\text{ES}}(\mathbf{Z})\right]^{-\mathbf{2.83}}. \tag{38}$$

For $\Delta t = 80$ min, the probability density distribution $p(Z)$ of CSI300 is

$$\mathbf{p}(\mathbf{Z}) = \left[\mathbf{0.30} + \mathbf{22.66Z} - \mathbf{1.59g}^{\text{Tail}}(\mathbf{Z}) - \mathbf{174.47g}^{\text{ES}}(\mathbf{Z})\right]^{-\mathbf{2.38}}. \tag{39}$$

As can be seen in Table 2 (second column), with the increase of time lags (from 10 to 80 minutes), the kurtosis values of CSI 300 index data decrease as they should. This corresponds to the decrease of tail thickness as the time lags increase. From Table 3 column two, we can see that the power-law exponents tend to decrease with the increase of time lags (from 10 to 80 min). We note that the rate of return $Z(t)$ for the stock market index is always smaller than 1

$(Z(t) < 1)$ and in this areas $Z^{-\alpha} > Z^{-\beta}$ for $\alpha > \beta$. For clearer exhibition of the dependence relationship of the tail thickness on the tail exponent, please see Figure 3. Thus, with the increase of the time lags (from 10 to 80 min), the distribution becomes less leptokurtic, and the tail exponent should decrease. This is consistent with our empirical results using the CSI 300 index data as shown in Tables 2 and 3 where the tail exponent decreases from 4.55 to 2.38. Ultimately, for the sufficiently large time lags (decades ago, it was many weeks; nowadays, due to much faster information transmission in the contemporary world, it is likely to take much less time), it approaches the normal distribution as consistent with the central limit theorem (CLT).

This effect can also be interpreted in terms of the Varma entropy. Varma entropy H_{ab} is proper to $\ln \int_{-\infty}^{\infty} p(x)^{a+b-1} dx$:

$$\mathbf{H_{ab} \sim \ln \int_{-\infty}^{\infty} p(x)^{a+b-1} dx}. \tag{40}$$

As $a + b$ is set equal to $2q - 1/q$, we have

$$\mathbf{a + b - 1 = 1 - \frac{1}{q}}. \tag{41}$$

Therefore, Varma entropy H_{ab} is proper to $\ln \int_{-\infty}^{\infty} p(x)^{1-1/q} dx$:

$$\mathbf{H_{ab} \sim \ln \int_{-\infty}^{\infty} p(x)^{1-1/q} dx}, \tag{42}$$

where q is the distribution tail power-law exponent of the probability density distribution $p(x)$ as in equation (25).

The limiting condition gives $q \geq 2$; thus, when q becomes smaller, $(1 - 1/q)$ becomes smaller. As $0 < p(x) < 1$, smaller exponent $(1 - 1/q)$ leads to higher value for $p(x)^{1-1/q}$. In other words, when power-law exponent q decreases with the increase of return lag Δt, Varma entropy H_{ab} becomes larger. When Varma entropy H_{ab} reaches its maximum value, the system reaches its equilibrium as a stable distribution. This is consistent with the principle of maximum entropy as entropy tends to increase when the system approaches its equilibrium value.

4. Robustness Tests

In this section, we apply our model to the S&P 500 of the USA stock market and different stock price indices in China's A-share market for robustness tests.

4.1. Robustness Tests of S&P 500 Index. In order to test whether the conclusions we draw are still robust for a mature financial market, we use the high-frequency data of S&P 500 in 2018 to calibrate our theoretical model. The results are exhibited in Table 4.

As can be seen in Table 4, the tail region of the return distribution is a power-law distribution with a very high R^2, which indicates that the power-law distribution can describe the tail region of the short-time interval return distribution well. Most of the power-law orders are between −2 and −7. When the time interval increases, the power-law exponents are most likely to decrease. With the calculated value-at-risk and expected shortfall, we numerically solve the four

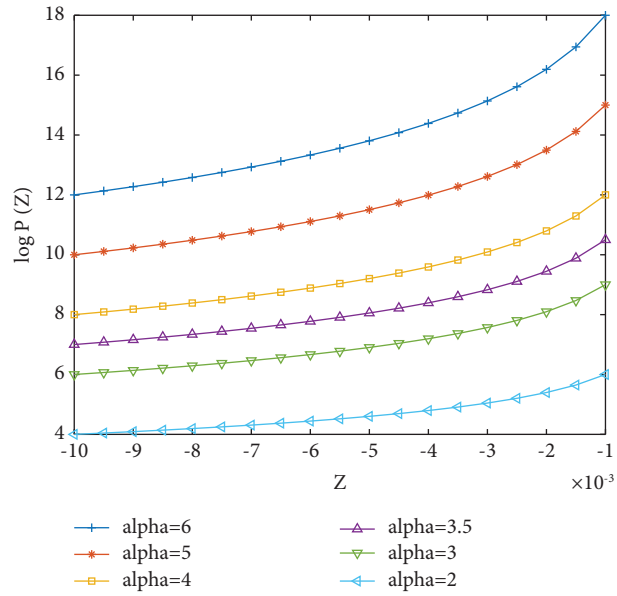

Figure 3: The dependence of tail thickness of return on tail exponent.

Table 4: Power-law distribution of return distribution of S&P 500.

Variable	R^2	Q	$\overline{\lambda_0}$	$\overline{\lambda_1}$	$\overline{\gamma}^{\text{Tail}}$	$\overline{\gamma}^{\text{ES}}$
$\Delta t = 10$ min	0.9059	6.2323	0.45	37.34	−0.14	−139.80
$\Delta t = 20$ min	0.9660	6.4678	0.49	27.14	−0.15	−103.53
$\Delta t = 30$ min	0.9789	3.9423	0.34	28.28	−0.35	−133.50
$\Delta t = 40$ min	0.9741	4.2597	0.37	24.64	−0.30	−109.20
$\Delta t = 50$ min	0.9854	3.9922	0.36	22.94	−0.38	−108.61
$\Delta t = 60$ min	0.9798	3.0018	−0.14	−12.30	0.29	66.53
$\Delta t = 70$ min	0.9959	3.4815	0.34	21.33	−0.49	−108.72
$\Delta t = 80$ min	0.9733	3.0954	0.31	21.80	−0.19	19.44

[1]*Note.* The data used are S&P 500 index of 2018 obtained from Wind.

Lagrangian multipliers $\overline{\lambda_0}$, $\overline{\lambda_1}$, $\overline{\gamma}^{\text{Tail}}$, and $\overline{\gamma}^{\text{ES}}$ and exhibit them in Table 4. In this way, we have used Varma entropy with VaR and ES constraints to find the numerical form of probability density distribution for high-frequency data of S&P 500.

For $\Delta t = 10$ min, the probability density distribution $p(Z)$ of the S&P 500 index is

$$\mathbf{p(Z) = \left[0.45 + 37.34Z - 0.14g^{Tail}(Z) - 139.80g^{ES}(Z)\right]^{-6.23}}. \tag{43}$$

For $\Delta t = 20$ min, the probability density distribution $p(Z)$ of the S&P 500 index is

$$\mathbf{p(Z) = \left[0.49 + 27.14Z - 0.15g^{Tail}(Z) - 103.53g^{ES}(Z)\right]^{-6.47}}. \tag{44}$$

For $\Delta t = 30$ min, the probability density distribution $p(Z)$ of the S&P 500 index is

$$\mathbf{p(Z) = \left[0.34 + 28.28Z - 0.35(Z) - 133.50g^{ES}(Z)\right]^{-3.94}}. \tag{45}$$

For $\Delta t = 40$ min, the probability density distribution $p(Z)$ of the S&P 500 index is

$$\mathbf{p}(\mathbf{Z}) = \left[\mathbf{0.37} + \mathbf{24.64Z} - \mathbf{0.30g}^{\mathrm{Tail}}(\mathbf{Z}) - \mathbf{109.20g}^{\mathrm{ES}}(\mathbf{Z})\right]^{-\mathbf{4.26}}. \tag{46}$$

For $\Delta t = 50$ min, the probability density distribution $p(Z)$ of the S&P 500 index is

$$\mathbf{p}(\mathbf{Z}) = \left[\mathbf{0.36} + \mathbf{22.94Z} - \mathbf{0.38g}^{\mathrm{Tail}}(\mathbf{Z}) - \mathbf{108.61g}^{\mathrm{ES}}(\mathbf{Z})\right]^{-\mathbf{3.99}}. \tag{47}$$

For $\Delta t = 60$ min, the probability density distribution $p(Z)$ of the S&P 500 index is

$$\mathbf{p}(\mathbf{Z}) = \left[-\mathbf{0.14} - \mathbf{12.30Z} + \mathbf{0.29g}^{\mathrm{Tail}}(\mathbf{Z}) + \mathbf{66.53g}^{\mathrm{ES}}(\mathbf{Z})\right]^{-\mathbf{3.00}}. \tag{48}$$

For $\Delta t = 70$ min, the probability density distribution $p(Z)$ of the S&P 500 index is

$$\mathbf{p}(\mathbf{Z}) = \left[\mathbf{0.34} + \mathbf{21.33Z} - \mathbf{0.49g}^{\mathrm{Tail}}(\mathbf{Z}) - \mathbf{108.72g}^{\mathrm{ES}}(\mathbf{Z})\right]^{-\mathbf{3.48}}. \tag{49}$$

For $\Delta t = 80$ min, the probability density distribution $p(Z)$ of the S&P 500 index is

$$\mathbf{p}(\mathbf{Z}) = \left[\mathbf{0.31} + \mathbf{21.80Z} - \mathbf{0.19g}^{\mathrm{Tail}}(\mathbf{Z}) + \mathbf{19.44g}^{\mathrm{ES}}(\mathbf{Z})\right]^{-\mathbf{3.10}}. \tag{50}$$

4.2. Robustness Tests of the Shanghai Composite Index. We also calibrate our theoretical model using different stock price indices in China's A-share market, namely, the Shanghai Composite index. The results are exhibited in Table 5.

As can be seen in Table 5, the tail region of the return distribution is a power-law distribution with very high R^2, which indicates that the power-law distribution can describe the tail region of the short-time interval return distribution well. Most of the power-law orders are between −2 and −7. When the time interval increases, the power-law exponents are most likely to decrease. We also exhibit the numerical results of the four Lagrangian multipliers $\overline{\lambda_0}$, $\overline{\lambda_1}$, $\overline{\gamma}^{\mathrm{Tail}}$, and $\overline{\gamma}^{\mathrm{ES}}$. With the solved parameters, we can write the numerical form of probability density distribution for high-frequency data of the Shanghai Composite index.

Thus, for $\Delta t = 10$ min, the probability density distribution $p(Z)$ of the Shanghai Composite index is

$$\mathbf{p}(\mathbf{Z}) = \left[\mathbf{0.34} + \mathbf{35.36Z} - \mathbf{0.40g}^{\mathrm{Tail}}(\mathbf{Z}) - \mathbf{192.09g}^{\mathrm{ES}}(\mathbf{Z})\right]^{-\mathbf{4.28}}. \tag{51}$$

For $\Delta t = 20$ min, the probability density distribution $p(Z)$ of the Shanghai Composite index is

$$\mathbf{p}(\mathbf{Z}) = \left[\mathbf{0.44} + \mathbf{24.29Z} - \mathbf{0.32g}^{\mathrm{Tail}}(\mathbf{Z}) - \mathbf{117.99g}^{\mathrm{ES}}(\mathbf{Z})\right]^{-\mathbf{5.36}}. \tag{52}$$

For $\Delta t = 30$ min, the probability density distribution $p(Z)$ of the Shanghai Composite index is

Table 5: Power-law distribution of return distribution of Shanghai Composite index.

Variable	R^2	q	$\overline{\lambda_0}$	$\overline{\lambda_1}$	$\overline{\gamma}^{\mathrm{Tail}}$	$\overline{\gamma}^{\mathrm{ES}}$
$\Delta t = 10$ min	0.7706	4.2815	0.34	35.36	−0.40	−192.09
$\Delta t = 20$ min	0.9905	5.3601	0.44	24.29	−0.32	−117.99
$\Delta t = 30$ min	0.9944	5.0466	0.44	21.24	−0.42	−48.94
$\Delta t = 40$ min	0.9942	4.1136	0.39	20.74	−0.49	−112.10
$\Delta t = 50$ min	0.9972	4.0104	0.39	19.21	−0.54	−106.29
$\Delta t = 60$ min	0.9984	3.0620	0.32	20.76	−0.78	−128.03
$\Delta t = 70$ min	0.9942	2.4848	0.28	23.46	−1.30	−173.84
$\Delta t = 80$ min	0.9983	2.1926	0.32	29.76	1.46	182.78

[1]*Note*. The data used are the Shanghai Composite index of 2018 obtained from Wind.

$$\mathbf{p}(\mathbf{Z}) = \left[\mathbf{0.44} + \mathbf{21.24Z} - \mathbf{0.42}(\mathbf{Z}) - \mathbf{48.94g}^{\mathrm{ES}}(\mathbf{Z})\right]^{-\mathbf{5.05}}. \tag{53}$$

For $\Delta t = 40$ min, the probability density distribution $p(Z)$ of the Shanghai Composite index is

$$\mathbf{p}(\mathbf{Z}) = \left[\mathbf{0.39} + \mathbf{20.74Z} - \mathbf{0.49g}^{\mathrm{Tail}}(\mathbf{Z}) - \mathbf{112.10g}^{\mathrm{ES}}(\mathbf{Z})\right]^{-\mathbf{4.11}}. \tag{54}$$

For $\Delta t = 50$ min, the probability density distribution $p(Z)$ of the Shanghai Composite index is

$$\mathbf{p}(\mathbf{Z}) = \left[\mathbf{0.39} + \mathbf{19.21Z} - \mathbf{0.54g}^{\mathrm{Tail}}(\mathbf{Z}) - \mathbf{106.29g}^{\mathrm{ES}}(\mathbf{Z})\right]^{-\mathbf{4.01}}. \tag{55}$$

For $\Delta t = 60$ min, the probability density distribution $p(Z)$ of the Shanghai Composite index is

$$\mathbf{p}(\mathbf{Z}) = \left[\mathbf{0.32} + \mathbf{20.76Z} - \mathbf{0.78g}^{\mathrm{Tail}}(\mathbf{Z}) - \mathbf{128.03g}^{\mathrm{ES}}(\mathbf{Z})\right]^{-\mathbf{3.06}}. \tag{56}$$

For $\Delta t = 70$ min, the probability density distribution $p(Z)$ of the Shanghai Composite index is

$$\mathbf{p}(\mathbf{Z}) = \left[\mathbf{0.28} + \mathbf{23.46Z} - \mathbf{1.30g}^{\mathrm{Tail}}(\mathbf{Z}) - \mathbf{173.84g}^{\mathrm{ES}}(\mathbf{Z})\right]^{-\mathbf{2.48}}. \tag{57}$$

For $\Delta t = 80$ min, the probability density distribution $p(Z)$ of the Shanghai Composite index is

$$\mathbf{p}(\mathbf{Z}) = \left[\mathbf{0.32} + \mathbf{29.76Z} + \mathbf{1.46g}^{\mathrm{Tail}}(\mathbf{Z}) + \mathbf{182.78g}^{\mathrm{ES}}(\mathbf{Z})\right]^{-\mathbf{2.19}}. \tag{58}$$

Overall, by empirical analysis, it is proved that the tail region of the return distribution is a power-law distribution. By maximizing mean-VaR-ES constraints, we can give the concrete numerical form of the probability density distribution of high-frequency stock market indexes, which are more theoretically reasonable and consistent with real-world characteristics. This conclusion is robust for data of different stock price indices in China's A-share market and for mature capital in developed countries represented by the S&P 500 of the United States.

5. Conclusions

It is crucial for financial investors to assess properly the risk of any prospective investment. Therefore, modeling accurately the probability density distribution function of financial assets is a vital issue in the field of risk management.

Many scholars have proved empirically that the distribution of return in stock markets does not obey Gaussian distribution [33] and many stock indices do not follow the random walk [1]. The distributions of stock price returns drop off more slowly than the normal distributions [32]. For a stock market with a heavy tail in return distributions, it is necessary to use a new uncertainty measure that does not depend on a particular distribution. Therefore, we would use entropy, which can be applied to measure uncertainty in probability theory [31], to model the non-Gaussian distribution.

By maximizing the Varma entropy with mean-VaR-ES constraints, we obtained the probability distribution of stock return in the tail region and deduced theoretically that the tail of stock return distribution is a power law. Since the volatility of the real stock portfolio may be stochastic, using the mean-VaR-ES constraints to maximize the Varma entropy effectively avoids the problem of assuming that the variance is a constant value under the traditional mean-variance constraint. In this way, the deduced probability density distribution of return is more theoretically reasonable and more consistent with the real market.

Using high-frequency data from China's stock markets, we calibrate our theoretical model and give the concrete form of probability density distribution $p(x)$ for different time intervals. We find that the tail region of the stock market index return distribution is a power law with most of the power-law orders between −2 and −7. With the increase of the time interval of return lag, the power-law exponents mostly tend to decrease. This is consistent with the central limit theorem as with the increase of the time lags, the distribution becomes less leptokurtic, and for the sufficiently large time lags, it approaches the normal distribution. With the increase of the time interval of return lag, the power-law exponents mostly tend to decrease. This is consistent with the principle of maximum entropy as entropy tends to increase when the system approaches its equilibrium value. With the calculated mean value of the return, the value-at-risk, and the expected shortfall, we calculate the four parameters $\overline{\lambda_0}$, $\overline{\lambda_1}$, $\overline{\gamma}^{\text{Tail}}$, and $\overline{\gamma}^{\text{ES}}$ in the probability density distribution under the mean-VaR-ES constraints and thus give the numerical form of probability density distribution for different stock market indices with different time intervals. We use different stock price indices in China's A-share market and stock market index from the mature capital market represented by the S&P 500 of the United States to calibrate the Varma entropy. The results show that our conclusions are robust for different stock markets.

Two groups may benefit from our results, namely, theoretical researchers and investment practitioners. For theoretical researchers, our model gives a complementary insight into what leads to the heavy tails observed in financial fluctuations. Besides, we also give a more theoretical explanation to the phenomenon that with the increase of the time interval of return lag, the power-law exponents mostly tend to decrease. Our research results can also benefit investment practitioners with a decision-making basis. However, further theoretical and empirical analyses are still needed. Further studies can be carried out by the following directions. First, studies may be carried out to further explore the deep meaning of the power-law parameter q and find more economic explanation for the mechanism leading to the power-law distribution of stock price fluctuations on small time scales. Second, researchers can also extend the idea with the maximum entropy principle to derive distribution for other financial assets and calibrate the model using real-world data.

Data Availability

The data used to support the findings of this study are available from the corresponding author upon request.

Disclosure

The funders had no role in the design of the study; in the collection, analyses, or interpretation of data; in the writing of the manuscript; or in the decision to publish the results.

Conflicts of Interest

The authors declare that they have no conflicts of interest.

Authors' Contributions

C.L. performed the formal analysis of the investigation, the methodology, and the software. C.L. and C.C. wrote the first draft of the paper and reviewed and edited the paper. All authors have read and agreed to the published version of the manuscript.

Acknowledgments

This research was supported by the China Postdoctoral Science Foundation (Grant no. 2021M700398) and the Fundamental Research Funds for the Central Universities (Grant no. FRF-TP-22-059A1).

References

[1] R. Dias, N. Teixeira, V. Machova, P. Pardal, J. Horak, and M. Vochozka, "Random walks and market efficiency tests: evidence on US, Chinese and European capital markets within the context of the global Covid-19 pandemic," *Oecon. Copernic.*, vol. 11, no. 4, pp. 585–608, 2020.

[2] R. N. Mantegna and H. E. Stanley, "Scaling behaviour in the dynamics of an economic index," *Nature*, vol. 376, pp. 46–49, 1995.

[3] J. Hull and A. White, "The pricing of options with stochastic volatilities," *The Journal of Finance*, vol. 42, pp. 281–300, 1987.

[4] R. F. Engle, "Autoregressive conditional heteroscedasticity with estimates of the variance of United Kingdom inflation," *Econometrica*, vol. 50, no. 4, pp. 987–1007, 1982.

[5] T. Bollerslev, "Generalized autoregressive conditional heteroskedasticity," *J.Econometrics*, vol. 31, no. 3, pp. 307–327, 1986.

[6] J. P. Bouchaud, "Power-laws in economy and finance: some ideas from physics," 2000, https://arxiv.org/abs/cond-mat/0008103.

[7] B. B. Mandelbrot, "The variation of certain speculative prices," *Journal of Business*, vol. 36, pp. 394–419, 1963.

[8] C. Liu and C. Chang, "Combination of transition probability distribution and stable Lorentz distribution in stock markets," *Physica A: Statistical Mechanics and its Applications*, vol. 565, Article ID 125554, 2021.

[9] P. Gopikrishnan, M. Meyer, L. A. N. Amaral, and H. E. Stanley, "Inverse cubic law for the distribution of the stock price variations," *The European Physical Journal B*, vol. 3, pp. 139-140, 1998.

[10] V. Plerou, P. Gopikrishnan, L. A. N. Amaral, M. Meyer, and H. E. Stanley, "Scaling of the distribution of price fluctuations of individual companies," *Physics Reviews E.*, vol. 60, pp. 6519–6529, 1999.

[11] P. Gopikrishnan, V. Plerou, L. A. N. Amaral, M. Meyer, and H. E. Stanley, "Scaling of the distribution of fluactuations of financial market indices," *Physics Review E.*, vol. 60, pp. 5305–5316, 1999.

[12] M. Wątorek, J. Kwapień, and S. Drożdż, "Financial return distributions: past, present, and COVID-19," *Entropy*, vol. 23, p. 884, 2021.

[13] T. Lux, "The stable Paretian hypothesis and the frequency of large returns: an examination of major German stocks," *Applied Financial Economics*, vol. 6, pp. 463–475, 1996.

[14] D. Makowiec and P. Gnaciński, "Fluctuations of WIG-the index of Warsaw stock exchange. Preliminary studies," *Acta Physica Polonica B*, vol. 32, pp. 1487–1500, 2001.

[15] S. Sinha and R. K. Pan, "The power (law) of Indian markets: analysing NSE and BSE trading statistics," in *Econophysics of Stock and Other Markets. Proc. Econophys-Kolkata II*, A. Chatterjee and B. K. Chakrabarti, Eds., Springer, Berlin/Heidelberg, Germany, 2006.

[16] G. Oh, S. Kim, and C.-J. Um, "Statistical properties of the returns of stock prices of international markets," 2006, https://arxiv.org/abs/physics/0601126.

[17] R. Rak, S. Drożdż, and J. Kwapień, "Nonextensive statistical features of the Polish stock market fluctuations," *Physica A: Statistical Mechanics and its Applications*, vol. 374, pp. 315–324, 2007.

[18] G.-F. Gu and W.-X. Zhou, "Statistical properties of daily ensemble variables in the Chinese stock markets," *Physica A: Statistical Mechanics and its Applications*, vol. 383, pp. 497–506, 2007.

[19] C. Eom, T. Kaizoji, and E. Scalas, "Fat tails in financial return distributions revisited: evidence from the Korean stock market," *Physica A: Statistical Mechanics and its Applications*, vol. 526, Article ID 121055, 2019.

[20] G. C. Philippatos and C. J. Wilson, "Entropy, market risk, and the selection of efficient portfolios," *Applied Economics*, vol. 4, pp. 209–220, 1972.

[21] J. P. Xu, X. Y. Zhou, and D. D. Wu, "Portfolio selection using λ mean and hybrid entropy," *Annals of Operations Research*, vol. 185, pp. 213–229, 2011.

[22] I. Usta and Y. M. Kantar, "Mean-variance-skewness-entropy measures: a multi-objective approach for portfolio selection," *Entropy*, vol. 13, pp. 117–133, 2011.

[23] P. Jana, T. K. Roy, and S. K. Mazumder, "Multi-objective possibilistic model for portfolio selection with transaction cost. J. Comput," *Applied Mathematics*, vol. 228, pp. 188–196, 2009.

[24] W. G. Zhang, Y. J. Liu, and W. J. Xu, "A possibilistic mean-semivariance-entropy model for multi-period portfolio selection with transaction costs," *European Journal of Operational Research*, vol. 222, pp. 341–349, 2012.

[25] R. X. Zhou, X. G. Wang, X. F. Dong, and Z. Zong, "Portfolio selection model with the measures of information entropy-incremental entropy-skewness," *Adv. Inf. Sci. Service Sci.*, vol. 5, pp. 853–864, 2013.

[26] X. X. Huang, "Mean-entropy models for fuzzy portfolio selection," *IEEE Transactions on Fuzzy Systems*, vol. 16, pp. 1096–1101, 2008.

[27] W. Rödder, I. R. Gartner, and S. Rudolph, "An entropy-driven expert system shell applied to portfolio selection," *Expert Systems with Applications*, vol. 37, pp. 7509–7520, 2010.

[28] S. G. Anton and A. E. Afloarei Nucu, "Sovereign Credit Default Swap and stock markets in central and eastern European countries: are feedback effects at work?" *Entropy*, vol. 22, p. 338, 2020.

[29] J. S. Ou, "Theory of portfolio and risk based on incremental entropy," *The Journal of Risk Finance*, vol. 6, no. 1, pp. 31–39, 2005.

[30] N. Lassance, "Minimum Rényi entropy portfolios," *Annals of Operations Research*, vol. 299, pp. 23–46, 2021.

[31] R. Zhou, R. Cai, and G. Tong, "Applications of entropy in finance: a review," *Entropy*, vol. 15, pp. 4909–4931, 2013.

[32] V. Plerou, P. Gopikrishnan, X. Gabaix, and H. E. Stanley, "On the origin of power-law fluctuations in stock prices," *Quantitative Finance*, vol. 4, pp. 11–15, 2004.

[33] A. Clauset, C. R. Shalizi, and M. E. Newman, "J. Power-law distributions in empirical data," *SIAM Review*, vol. 51, pp. 661–703, 2009.

[34] D. Geman, H. Geman, and N. N. Taleb, "Tail risk constraints and maximum entropy," *Entropy*, vol. 17, pp. 3724–3737, 2015.

[35] C. Liu, C. Chang, and Z. Chang, "Maximum Varma entropy distribution with conditional value at risk constraints," *Entropy*, vol. 22, p. 663, 2020.

[36] P. A. Rappoport, "New approach: average shortfall," Technical Report, Scientific Research Publishing, Wuhan, China, 1993.

[37] P. Artzner, F. Delbaen, J.-M. Eber, and D. Heath, "Thinking coherently," *Risk J*, vol. 10, pp. 68–71, 1997.

[38] P. Artzner, F. Delbaen, J.-M. Eber, and D. Heath, "Coherent measures of risk," *Mathematical Finance*, vol. 9, pp. 203–228, 1999.

[39] R. S. Varma, "Generalizations of Rényi's entropy of order α," *Journal of Mathematical Sciences*, vol. 1, pp. 34–48, 1966.

[40] C. Sun, Z. Lin, M. Vochozka, and Z. Vincurova, "Digital transformation and corporate cash holdings in China's A-share listed companies," *Oecon. Copernic.*, vol. 13, no. 4, pp. 1081–1116, 2022.